Stability of Two-Dimensional Foams in Langmuir Monolayers

E. K. Mann* and S. V. Primak

Department of Physics, Kent State University, P.O. Box 5190, Kent, Ohio 44242-0001

(Received 18 May 1999)

Two-dimensional foams within a polymer Langmuir monolayer show markedly different stability on two different substrates. This contrast is used to explore foam stability in Langmuir layers. The relaxation of 2D isolated droplets allows both the measurement of the line tension and the assessment of hydrodynamics. Surface potential measurements assess long-range electrostatic repulsion due to alignment of molecular dipoles at the surface. The surface potential difference between gaseous and liquid polymer domains is larger, by more than a factor of 7, where foams are stable than where they are not.

PACS numbers: 82.70.Rr, 68.55.–a, 83.70.Hq

Three-dimensional (3D) foams and emulsions are the stuff of everyday experience, on top of beer or dessert, in the wash water for dishes or laundry, or on the seashore. Their stability or prevention is crucial to gustatory pleasure, to the working of washing machines, and to chemical processing, where foaming is often an undesirable side effect. Such foams display complex rheologies and time evolution, currently a focus of both theoretical and experimental activity [1–3].

The collapse of the foam into separate liquid and gas phases is inhibited, in 3D foams, by surface-active agents [4]. Both static and dynamic factors play important roles [5]. An ionic surfactant provides electrostatic repulsion between the layers sandwiching the film, to counteract the van der Waals attraction across the film. Surfactant layers or micelles within the film provide steric repulsion. The dynamic response of the surfactant layer, characterized by frequency-dependent surface viscosities and elasticities, helps the film resist shocks and the draining of fluid through the films.

Foam analogs in Langmuir monolayers have served as model systems to explore the evolution of foams with time [3], much-studied theoretically in the 2D case [1]. A Langmuir monolayer consists of an insoluble surface-active agent spread at the air-water interface into a film everywhere one molecule thick or less. Movement within Langmuir layers is confined to the 2D plane of the substrate; in this sense, these are true 2D systems. At low concentrations, such monolayers often phase separate into a dilute "gaseous" phase and a much denser "liquid" phase. Very often, "foams" form, in which gaseous bubbles are surrounded by thin films of liquid phase. The films come together at three-film contact points, with average angles of 120° between films (see Fig. 1): these are analogous to plateau borders in 3D foams. While such foams are very commonly observed in Langmuir monolayers, the reason for their long-term stability remains unclear. There are usually no obvious line-active agents, as there must be in the 3D case. Even undetectable amounts of impurities could play this role [6], but they may not be necessary for 2D film stability.

Both static and dynamic factors must be considered for roles in stabilizing the films between monolayer domains. Breakup mechanisms are similar to the 3D case. However, the hydrodynamics during the breakup process are significantly different than in 3D foams, which may be one source of 2D foam stability [7]. A further major difference from the 3D films is that the intrinsic symmetry breaking of the air/water interface aligns molecular dipoles perpendicularly to that interface. There is a net dipole moment difference between two different phases of the monolayer, which provides a net electrostatic repulsion across films between phases [Fig. 2(a)], stabilizing the film. It has been suggested [8] that some 2D foams may be true equilibrium phases. Charged line-active agents would provide an additional source of electrostatic repulsion, but these are negligible since the micron thickness of the liquid film separating gaseous domains is much greater than the fluid Debye length.

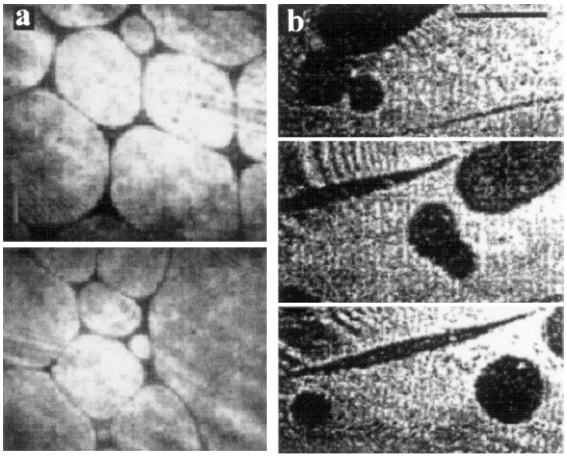

FIG. 1. Typical configurations for phase-separated monolayers of PDMS on top of: (a) water; the dilute, gaseous domains are brighter than the denser, liquid domains; (b) a homogeneous AOT layer, on an AOT solution at ~3 cmc, with 3.5 s intervals between images; gaseous domains are darker than the liquid domains. Image artifacts include the Gaussian beam profile and interference fringes. Bars represent 50 μm.

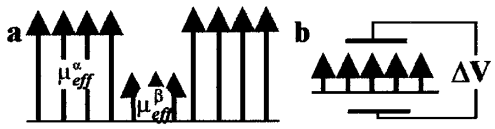

FIG. 2. Schematics: (a) The difference in the effective dipolar surface density μ_{eff} of phases α and β leads to repulsion between two domains of phase α. (b) The surface potential ΔV is the drop in voltage between two capacitor plates across the interface, due to the effective dipole surface density. ΔV changes between the two phases of (a). ΔV was determined under conditions such that the domains were sufficiently large for the measurement of each phase separately.

Studying the stability of foams in Langmuir monolayers has been difficult due to the lack of systematically variable parameters. For 3D films the major variable parameters are the nature and concentration of the surface-active agent and the ionic strength of the solution, governing the electrostatic interactions between surfactant layers sandwiching the thin films. In the absence of obvious line-active agents, such control is difficult to envisage in the monolayer case.

Here we consider two closely related Langmuir monolayer systems, both of the same polymer, poly(dimethylsiloxane) or PDMS [9], but spread on two different substrates. Previous work [10] on these Langmuir monolayers, using primarily neutron reflectivity, demonstrated that when small quantities, ~ 1 mg/m^2, of the polymer are deposited on the surface of water, the polymer spreads to form a layer roughly one monomer thick. The studies [10] demonstrated that such a layer forms on *top* of the homogenous surfactant layer covering the surface of concentrated sodium di(2-ethylhexyl)sulfosuccinate (AOT) solutions [11], without changing the AOT layer and without mixing in it.

The surfactant layer and the pure water surface furnish our two substrates. With less than ~ 0.6 mg/m^2 of polymer, the polymer layer separates into liquid and gas phases, as demonstrated [12] by Brewster angle microscopy (BAM). Under undisturbed conditions, phase domains are very large but if the surface is disturbed, by changing the temperature or by decreasing the humidity, gas holes develop at the edge of liquid domains in both systems (Fig. 1). These holes form stable foam morphologies on the pure water [Fig. 1(a)] substrate but never on the surfactant substrate. There, a film between two gaseous domains sufficiently close together breaks, leading to coalescence of the domains [Fig. 1(b)]. Such film breakage was never observed on the first substrate. Also common on the second substrate [Fig. 1(b)], but never observed on the first, were lines of undulating thickness, reminiscent of the capillary wave mechanism for film breakup [13]. The similarity of the two systems, with their very different behavior with respect to foam stability, allows us to explore experimentally three of the factors that may most influence foam stability in general: the line tension, the hydrodynamics within the 2D system, and the electrostatic repulsion due to the dipole density difference between gaseous and liquid phases.

All measurements were done in a water-saturated atmosphere under plastic or Plexiglas covers. Surface pressure measurements were performed via the Wilhelmy method, with an accuracy of ~ 0.1 mN/m. Water was purified using Millipore MilliQ systems. Spreading solutions for the polymer were made with hexane (Merck or Fisher HPLC Grade). For the surface potential measurements, adding 1 mM NaCl (Fisher, certified ACS grade) increased the conductivity of the pure water solution.

The line tension and the hydrodynamics associated with domains on both substrates were explored through the relaxation of isolated domains, using BAM [14] for visualization. After being deformed by shear through the liquid substrate, the domains relaxed back towards an equilibrium circular shape. Relaxation is driven by the minimization of the line tension λ and braked by viscosity both within the surface layer (η_s) and within the bulk liquid (η_b), which is dragged along with the monolayer. For small deformations, the relaxation is exponential, defining a relaxation time t_c. If the viscosity within the bulk liquid dominates the energy losses during relaxation, $t_c = 5\pi\eta_b r^2/16\lambda$ [15], where $r = (A/\pi)^{1/2}$ is the equilibrium domain radius; the area A of that domain was found to be constant during the relaxation. If viscous losses within the surface dominate relaxation, $t_c = \eta_s r/\lambda$. Measurements of the characteristic relaxation times were reported earlier for polymer domains on water substrates, increasing η_b by the addition of glucose or glycerol [16]. Here the measurements are extended to polymer domains on the AOT solution substrate.

For the water/glycerol substrate, the relaxation times followed the relation $t_c \propto \eta_b^{1\pm0.1} r^{1.9\pm0.2}$, indicating that indeed the bulk viscosity dominates the hydrodynamics, over a range of 20 in domain size and a factor of 75 in bulk viscosity [16]. The inverse relaxation times, scaled by the known bulk viscosity and domain sizes, then give an estimate of the line tension on the water substrates as shown in Fig. 3. The present measurements for the polymer on top of the AOT substrate (Fig. 3) follow, within scatter, the measurements on the water substrates; $t_c \propto r^{2.0\pm0.1}$. This strongly suggests two crucial conclusions for the behavior of these monolayers. First, over the time and size scale explored in these measurements (0.1–100 s, 5–100 μm), the hydrodynamics are dominated by the viscosity of the bulk liquid. Neither surface viscosity nor any line elasticity or viscosity plays significant roles. This is true not only for the polymer layers on water but also on the AOT substrate. Second, the line tensions for polymer domains on the two substrates are very similar: The average values are 1.1 ± 0.3 pN on water compared to 1.37 ± 0.25 pN on the AOT substrate.

The difference in the effective dipole density μ_{eff} for the two phases was explored through surface potential

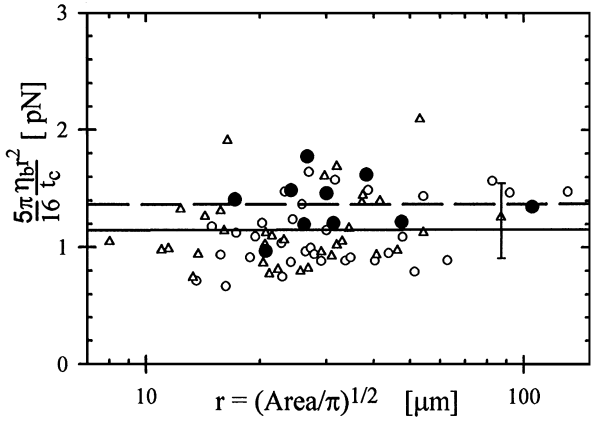

FIG. 3. The inverse relaxation time $1/t_c$ for PDMS liquid domains on: (○) water, (△) water/glycerol with bulk viscosity $\eta_b = (1.5-75)\eta_{\text{water}}$; see Ref. [16] for details. (●) AOT solutions, with $c_b \sim 3$ cmc. $1/t_c$ is normalized to give the line tension (see text). A representative error bar, due mostly to convection within the layer, is shown. The solid line is the average value on the water substrate, 1.1 pN; the dashed line is the average value on the AOT substrate 1.37 pN.

measurements. The drop in potential across the air-water interface, called the surface potential, is proportional to μ_{eff} for uncharged systems (see Fig. 2). In a continuum approximation, $\Delta V = \mu_{\text{eff}}/\varepsilon\varepsilon_0$, where ε is the local dielectric constant and ε_0 the dielectric constant of the vacuum [4]. Many groups [17] have shown that both hydrocarbon and end-group dipolar moments in the Langmuir monolayer can alter the surface potential. In seeking to interpret the surface potentials in terms of molecular dipole moments, the dielectric constant is often taken as unity ($\varepsilon_{\text{air}} = 1$). In fact, ε may vary between 80 (for water) and ≤ 2 (for dense hydrocarbon chains) within the interfacial region. However, to a first approximation, ε acts equivalently in ΔV and in long-range dipolar repulsion [12]. Surface potential measurements thus give a good measure of long-range repulsion within a monolayer. Indeed, these measurements correlate well with observed domain shape and behavior [18].

Surface potential and pressure measurements were done simultaneously using the KSV 5000 double-trough Langmuir-Blodgett system (KSV, Finland). With hydrophilic barriers, the compression/decompression isotherms showed no hysteresis, with pure water or with AOT solution substrates. The surface potential measurements (see Fig. 2) used the vibrating capacitor method, with an accuracy of 10 mV.

The surface potential ΔV is generally given with respect to the values measured on the substrate before addition of the monolayer, to compensate for potential drops across the electrode/solution and other junctions. The reference value is known to drift [4]. The surface potential drift in the absence of PDMS was explored for over 3 h, compared to the 35 min of the compression/decompression cycle. After substantial drifts within the first 15 min, the baseline could be determined within 5 mV for water and 20 mV for the AOT solutions.

Representative surface potential and surface pressure isotherms are given in Fig. 4 as a function of polymer surface concentration on the two substrates. The surface concentration ranges from the coexistence region, as demonstrated by BAM, through the region in which the polymer forms a compact, homogenous layer which then compresses. It is only as the homogeneous layer is compressed that the surface tension changes significantly. The boundary between the coexistence and homogeneous regions of the isotherms is indicated roughly on the figure. It is difficult to determine the boundary exactly with the very large phase domains.

In different runs, the PDMS spreading solution was deposited at different locations of the trough with respect to the vibrating electrode. The polymer remains near where it is deposited. We then expect the surface potential to vary between that of the gaseous domains and that of the liquid domains as these domains are pushed across the surface during compression. On the water substrate, we do indeed see quite abrupt variations in the potential within the coexistence region, between the value of the substrate and the value consistently found at the end of the coexistence region. At any one concentration in the coexistence region, both values are observed in different runs, demonstrating that domains are larger than the measurement electrode, ~4 cm. The extreme values give unambiguously the surface potential difference between the two types of domains. At the end of the coexistence regime, all potential isotherms reached a plateau value ~200 mV, in good agreement with a recent measurement using the vibrating electrode technique [19], but about

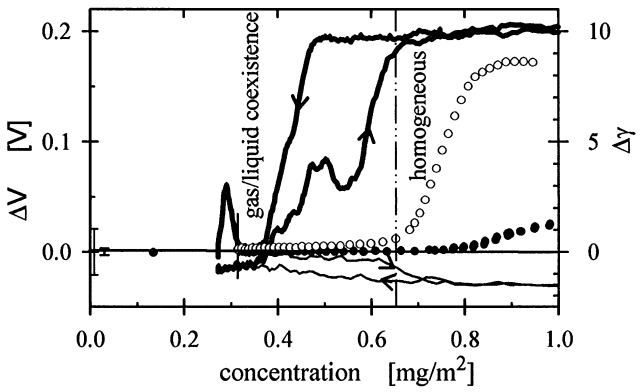

FIG. 4. Representative isotherms for the surface potentials ΔV (lines) and decrease in surface tension $\Delta\gamma$ (symbols), both with respect to the substrate values, as a function of PDMS surface concentration. Substrates: water (heavy line: $\Delta V \geq 0$; ○: $\Delta\gamma$) and AOT ($c_b \sim 3$ cmc; light line: $\Delta V \leq 0$; ●: $\Delta\gamma$) substrates. Vertical dashed line indicates approximate boundary between phase coexistence and a single condensed phase (BAM). Arrows indicate compression and decompression. Error bars near 0 indicate the observed range of ΔV in the 30 min preceding PDMS application.

50 mV higher than an earlier one [20] using the ionizing electrode method.

On the AOT substrate (Fig. 4), surface potential differences from the pure substrate through the coexistence region to the condensed polymer layer are small, near the limit of the available precision. We can certainly conclude that the surface potential difference between polymer liquid and polymer gaseous regions is <30 mV.

In summary, line tensions vary little between the two systems, on water compared to on AOT. The hydrodynamics, at least on the >5 μm and >0.1 s scale, are also equivalent on the two substrates, dominated by the bulk viscosity. Neither simple domain energetics nor dynamic effects, in draining the liquid between gaseous domains, for example, can account for the difference in foam stability. However, the surface potential difference between domains is >7 times larger on pure water substrates than on AOT substrates. We can conclude that the greatly increased stability of 2D foams on pure water substrates is due to electrostatic repulsion across foam films. The effect of this long-range repulsion on both the evolution and viscoelasticity of monolayer foams [1,3] should be considered. We also note the value of surface potential measurements in characterizing this long-range electrostatic repulsion. A molecular interpretation of the vastly different surface potentials of PDMS on water and on AOT remains to be developed.

S. Sahasithiwat and T. Srikhirin, of the Polymer Microdevices Laboratory (Case Western Reserve University), are thanked for their patient help with the surface potential measurements. E. K. M. would like to thank, as always, J. Meunier, of the L.P.S., l'Ecole Normale Supérieure, and S. Hénon, of the L.B.H.P., Université de Pairs VI et VII.

*Email address: mann@physics.kent.edu

[1] D. J. Durian, Phys. Rev. Lett. **75**, 4780 (1995); T. Okuzono and K. Kawasaki, Phys. Rev. E **51**, 1246 (1995); S. Hutzler, D. Weaire, and F. Bolton, Philos. Mag. B **71**, 277 (1995).

[2] A. A. el Kader and J. C. Earnshaw, Phys. Rev. Lett. **82**, 2610 (1999); R. Hohler, S. CohenAddad, and H. Hoballah, Phys. Rev. Lett. **79**, 1154 (1997).

[3] M. Dennin and C. M. Knobler, Phys. Rev. Lett. **78**, 2485 (1997); K. J. Stine, S. A. Rauseo, B. G. Moore, J. A. Wise, and C. M. Knobler, Phys. Rev. A **41**, 6884 (1990); B. Berge, J. A. Simon, and A. Libchaber, Phys. Rev. A **41**, 6893 (1990).

[4] A. W. Adamson and A. P. Gast, *Physical Chemistry of Surfaces* (Wiley, New York, 1997), 6th ed.

[5] R. J. Pugh, Adv. Colloid Interface Sci. **64**, 67 (1996); R. Aveyard and J. H. Clint, Curr. Opin. Colloid Interface Sci. **1**, 764 (1996).

[6] J. Lucassen, S. Akamatsu, and F. Rondelez, J. Colloid Interface Sci. **144**, 434 (1991).

[7] F. Brochard-Wyart, C.R. Acad. Sci. Paris II **311**, 295 (1990).

[8] K. Miyano and K. Tamada, Langmuir **8**, 160 (1992).

[9] The molecular weights of the PDMS samples were (a) $M_w = 10\,000$, $M_w/M_n = 1.13$ and (b) $M_w = 101\,000$, $M_w/M_n = 1.23$, both gifts from L. Lèger and P. Silberzan, and (c) $M_w = 10\,000$, $M_w/M_n = 1.06$, from Polymer Source, Inc., Quebec, Canada. Samples showed no significant behavioral differences.

[10] L. T. Lee, E. K. Mann, O. Guiselin, D. Langevin, B. Farnoux, and J. Penfold, Macromolecules **26**, 7046 (1993); E. K. Mann, L. T. Lee, S. Hénon, D. Langevin, and J. Meunier, Macromolecules **26**, 7037 (1993).

[11] The AOT, used at concentration $c_b \sim 2$ g/l or ~ 3 cmc, its critical micellar concentration, had two sources: (a) gift from Cyanamide (France); (b) Fluka, MicroSelect grade. Isotherms of PDMS on solutions of AOT from the two sources showed no significant differences.

[12] E. K. Mann, S. Hénon, D. Langevin, and J. Meunier, J. Phys. (Paris) II **2**, 1683 (1992).

[13] J. G. H. Joosten, in *Thin Liquid Films*, edited by I. B. Ivanov (Marcel Dekker, New York, 1988), p. 569.

[14] S. Hénon and J. Meunier, Rev. Sci. Instrum. **62**, 936 (1991); D. Honig and D. Mobius, J. Phys. Chem. **95**, 4590 (1991).

[15] H. A. Stone and H. M. McConnell, Proc. R. Soc. London A **448**, 97 (1995).

[16] E. K. Mann, S. Hénon, D. Langevin, J. Meunier, and L. Léger, Phys. Rev. E **51**, 5708 (1995).

[17] W. D. Harkins and E. K. Fischer, J. Chem. Phys. **1**, 852 (1933); T. Fort, Jr. and A. E. Alexander, J. Colloid Sci. **14**, 190 (1959); V. Vogel and D. Möbius, J. Colloid Interface Sci. **126**, 408 (1988) are examples.

[18] D. J. Benvegnu and H. M. McConnell, J. Phys. Chem. **96**, 6820 (1992); **97**, 6686 (1993).

[19] V. L. Shapovalov, Thin Solid Films, **327–329**, 816 (1998).

[20] M. K. Bernett and W. A. Zisman, Macromolecules **4**, 1 (1971).